Comparison of rapid techniques for classification of ground meat

Irene M. Nolasco-Perez [a], *Luiz A.C.M. Rocco* [a], *Jam P. Cruz-Tirado* [a], *Marise A.R. Pollonio* [b], *Sylvio Barbon, Jr.* [c], *Ana Paula A.C. Barbon* [d], *Douglas F. Barbin* [a,*]

[a] *Department of Food Engineering, University of Campinas (UNICAMP), Brazil*
[b] *Department of Food Technology, University of Campinas (UNICAMP), Brazil*
[c] *Department of Computer Science, Londrina State University (UEL), Brazil*
[d] *Department of Zootechnology, Londrina State University (UEL), Brazil*

Computer vision and near infrared spectroscopy are fast and non-invasive techniques currently available for processing control in the meat industry. These techniques can be used, either separately or combined, for on-line assessment of meat quality parameters. This study aimed to compare a portable near-infrared (NIR) spectrometer, near infrared hyperspectral imaging (NIR-HSI) and red, green and blue imaging (RGB-I) to differentiate ground samples from beef, pork and chicken meat; and to quantify amounts of each in mixtures. Chicken breast meat was adulterated with either pork leg meat or beef round meat from 0 to 50% (w/w). Partial Least Squares regression (PLSR) models were performed using full spectra and after selecting most important wavelengths. The best results were obtained with NIR-HSI, with coefficient of prediction (R^2_P) of 0.83 and 0.94, ratio performance to deviation (RPD) of 1.96 and 3.56, and ratio of error range (RER) of 10.0 and 18.1, for samples of chicken adulterated with pork and beef, respectively. In addition, the results obtained using NIR spectroscopy and RGB-I confirm that these techniques provide an alternative for rapid, on-line inspection of ground meat in the food industry.

Keywords:
authentication
food adulteration
process analytical technologies
chicken

1. Introduction

The poultry meat industry is increasing worldwide as poultry meat is considered an important component in healthy diets. The market becomes more demanding in quality, safety, environmental legislation, ethics, and sustainable production requirements. Therefore, quality control in the production supply chain of poultry meat is essential to ensure consumer confidence. Currently, meat and meat products adulteration with other meats or objectionable species is common in many countries (Ballin, Vogensen, & Karlsson, 2009). This practice can bring health risks (for instance: allergies and metabolomic disorders) (Woolfe & Primrose, 2004) and religious conflicts (Ballin, 2010).

* Corresponding author.
E-mail address: dfbarbin@unicamp.br (D.F. Barbin).

The meat industry is dynamic and complex, needing low-cost and environmentally friendly fast techniques to ensure the quality and authenticity of products. Near infrared spectroscopy (NIRS) is a promising technique for food authentication because it is fast, sensitive, reagent-free and can be used for process control in the industry in continuous food processing lines (Campos, Mussons, Antolin, Debán, & Pardo, 2017; Garcia-Martin, 2015; Martínez Gila, Cano Marchal, Gámez García, & Gómez Ortega, 2015; Massantini et al., 2017; Munir et al., 2017; Santos et al., 2016). NIRS has been demonstrated to be a reliable technique for food control and food authentication in different meat products: prediction of meat quality parameters (Barbin et al., 2015; Li et al., 2016; Wang, Peng, Sun, Zheng, & Wei, 2018), meat discrimination (Prieto et al., 2015), differentiation between fresh and frozen/thawed chicken (Grunert, Stephan, Ehling-Schulz, & Johler, 2016), adulteration of turkey meat (Alamprese, Amigo, Casiraghi, & Engelsen, 2016) and beef (Rady & Adedeji, 2018), classification of chicken breast fillets (Yang et al., 2018) and classification of different parts of chicken (Nolasco Perez et al., 2018).

Red, green and blue Imaging (RGB-I) is interesting for the meat industry for its simplicity, low cost, and non-destructive nature (Santos Pereira, Barbon, Valous, & Barbin, 2018). RGB images can be captured by digital cameras, webcams or scanners from computer vision systems (CVS), which usually contain a lighting system, camera, and image analysis software using a computer (Liu, Sun, Young, Bachmeier, & Newman, 2018). This technique allows the general colour and visual appearance of the sample to be determined (Barbin et al., 2016). RGB-I has been used to discriminate beef and pork (Arsalane, El Barbri, Rhofir, Tabyaoui, & Klilou, 2017), to predict pork colour attributes (Sun, Young, Liu, & Newman, 2018) and to classify and predict beef freshness (Arsalane et al., 2018).

Near infrared hyperspectral imaging (NIR-HSI) combines imaging and NIR spectroscopy, overcoming some limitations of these techniques when they are used individually (Feng, Makino, Oshita, & Garcia-Martin, 2018; Zheng, Li, Wei, & Peng, 2019). NIR-HSI provides simultaneous determination of physical and chemical properties of the sample, as well as their spatial distribution (Feng, Makino, Yoshimura et al., 2018; Riccioli, Pérez-Marín, & Garrido-Varo, 2018). Therefore, this technology is capable of identifying analytes that are not homogeneously distributed in the food matrix (Barreto, Cruz-Tirado, Siche, & Quevedo, 2018; Feng, Makino, Yoshimura et al., 2018). The capacity of NIR-HSI to identify chemical features has been used for identification of beef adulterated with chicken (Kamruzzaman, Makino, & Oshita, 2016), lamb adulterated with duck meat (Zheng et al., 2019), beef adulterated with chicken, pork meat and/or vegetable proteins (Rady & Adedeji, 2018), adulteration of fat content in chicken meat (Fernandes et al., 2019) and beef and horse meat discrimination (Arsalane et al., 2017).

Each of the three techniques has advantages and drawbacks. NIR spectroscopy provides spectral information but several measurements are necessary, while RGB-I provides spatial information in a limited number of wavelengths. Although NIR-HSI solves this drawback by combining spatial and spectral information, it is much more expensive than NIR spectroscopy or RGB-I. In general, the meat industry can use these technologies for meat authentication and routine mixture analyses in real time, according to their needs.

To the best of our knowledge, no work has reported identification and classification of chicken meat adulterated with pork comparing NIR-HSI, NIRS and RGB-I. Therefore, the main objective of the present study was to investigate and compare NIRS, NIR-HSI and RGB-I techniques for fast classification of pure chicken meat and chicken samples adulterated with beef or pork.

2. Material and methods

2.1. *Sample preparation*

Meat samples from breast (chicken), leg (pork) and round (beef) were used in the present research. This study consisted of two parts: first, 60 samples from three different species (20 chicken, 20 pork, 20 beef) were prepared and used for classification models.

Afterwards, 420 samples (210 samples adulterated with pork and 210 samples adulterated with beef) were prepared for prediction models, to quantify the amount of beef or pork added to chicken meat. Chicken meat was mixed with pork or beef in the range of 0–50% of mixtures, at intervals of approximately 2%. The samples were divided into two sample sets: the calibration (training) set containing 135 samples (in the range of 0–50% at approximately 2% increments) and prediction (test) set containing 75 samples (in the range of 0–48% at approximately 4% increments). Samples of each species were individually cut, weighed (totalling 20 g) and ground together in a meat processor. The ground samples were moulded in a circular glass (1.1 cm deep and 5 cm diameter).

2.2. *NIR spectroscopy*

NIR spectra were acquired in the range of 900–1700 nm at 3.51 nm intervals with 228 spectral bands using a portable spectrophotometer (NIRScan Nano, Texas Instruments, USA) in absorbance mode. The acquisition of the spectra was performed by direct contact in the same (central) region of each sample. Therefore, one spectrum was collected from each of the 60 pure samples and 420 adulterated samples.

2.3. *NIR hyperspectral imaging (NIR-HSI)*

Spectral images were recorded in the range of 900–2500 nm, at spectral intervals of 6 nm giving 256 spectral bands, in the reflectance mode at a scanning speed of 63.30 mm s^{-1}, using an NIR-HSI system (SisuCHEMA NIR/SWIR, Specim Ltd., FIN–90571 FINLAND). The system consisted of line scan spectrograph; a near infrared spectral camera (Specim – SisuCHEMA NIR XL, SPECIM Ltd, Finland), with a line scan detector of 320 pixels and spatial resolution of 623 μm; an OLE15 lens with 200 mm field of view and adductor, a diffuse illumination unit of 10 W halogen side reflector lamp Osram Ministar (Specim Ltda, Oulu, Finland), a sample tray platform, linear moving stage, and a computer supported with data

acquisition software ChemaDAQ (Specim Ltda, Oulu, Finland). The focal length for camera was 15 cm and frame rate was 100 fps. The calibrations for black reference and white reference were performed automatically by the system.

Hyperspectral images were manually segmented, isolating the region of interest of each sample (ground meat) from the background, for extraction of spectral information. The segmentation was carried out to obtain the average spectrum for each sample, using the EVINCE 2.0 software (UmBio AB, 2009).

2.4. *RGB-imaging (RGB-I)*

Images of ground samples were captured by a computer vision system previously described by Santos Pereira et al. (2018). The system consists of an illumination source of two LED lamps (Natural daylight, 100 W – Brazil), located at an angle of 45°, a digital camera (Sony, Japan) and chamber with matte black internal walls to reduce the shadowing effects. The camera settings for the images were: manual exposure with shutter speed of 1/60 s (zoom and flash off) and ISO number of 200.

2.4.1. *Image analysis and feature extraction*

Each colour image was pre-processed in MATLAB R2016a (Mathworks, USA), and the segmentation was carried out for extraction of the region of interest (ROI) by removing the background of the image. All images were separated into 3 images representing the absorption of the primary colours red, green and blue (RGB), subsequently converted to hue saturation value (HSV). Once the matrix to be analysed had been chosen, the Otsu method was used to transform the grayscale image (Mora & Fonseca, 2014; Otsu, 1979). After applying the Otsu method, a binarised image was obtained, and small objects were removed in the image to perfectly isolate the region of interest; thus, only the features of the samples were extracted. In total, 59 variables (9 variables from average of colour channel R, G, B, H, S, V, L*, a* and b*; 1 variable from average of binary image intensity; 28 variables from texture features of Gray Level Co-occurrence Matrix (GLCM), contrast, energy, correlation and homogeneity from R, G, B, H, V, S and binary, 21 variables from entropy, kurtosis, skewness from R, G, B, H, V, S and binary) were extracted for each image.

2.5. *Multivariate analyses*

Principal component analysis (PCA) was applied to the NIR spectra, NIR-HSI spectra and RGB-I data of the pure samples for classification of meat species (chicken, pork, and beef). Then, a few wavelengths were selected using the PCA loadings, and another PCA and linear discriminant analysis (LDA) was carried out using only the selected wavelengths. LDA discriminates functions to achieve maximum variation between classes and to minimise variation within each class (Pizarro, Rodríguez-Tecedor, Pérez-del-Notario, Esteban-Díez, & González-Sáiz, 2013).

Similarly, Partial Least Squares regression (PLSR) was carried out using all the wavelengths without any pre-processing and compared with information after Multiplicative Scatter Correction (MSC), Standard Normal Variate (SNV), 1st derivative, 2nd derivative. Each pre-processing technique was applied separately for comparison. Then, PLSR was developed in the pretreated data to verify the best result. Performance of the models was compared by root mean square error of calibration (RMSEC), cross-validation (RMSECV), and prediction (RMSEP), as well as the coefficient of determination of calibration (R^2_c), cross-validation (R^2_{cv}), and prediction (R^2_p); and finally, the ratio performance to deviation (RPD) and the ratio of error range (RER).

2.5.1. *Selection of most relevant wavelengths*

Selecting wavelengths is important to reduce the high dimensionality of the spectral data to increase processing speed and to reduce the cost of hardware configuration (Kamruzzaman, ElMasry, Sun, & Allen, 2012). Stepwise regression (Cluff et al., 2008) and PCA loadings for the pure samples and PLSR regression coefficients for the adulterated samples were used to select important wavelengths. Stepwise regression using forward selection with p-value of 0.25 of significance level was performed to identify which wavelengths were most relevant, using the program Minitab

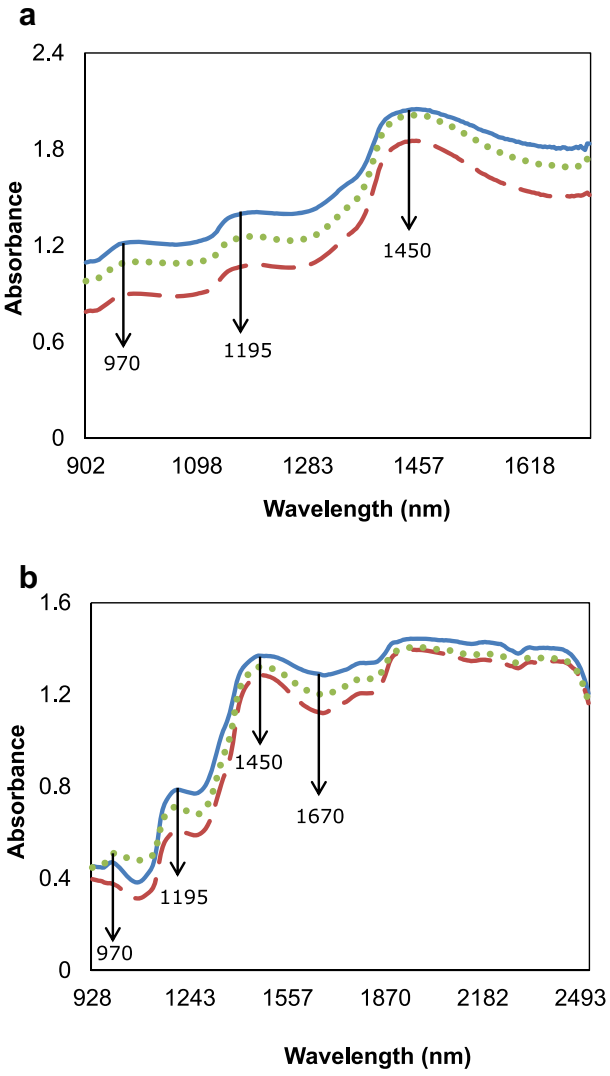

Fig. 1 – Average spectra of ground meat samples: (····) beef, (– –) pork and (—) chicken; acquired by: a) portable NIR spectrometer; b) NIR hyperspectral imaging system.

(Minitab 14 Inc., Release for WindowsTM, U.S.A.). This method begins with one wavelength and incorporates a new variable in the model at each iteration until a specified number of wavelengths is reached (Kamruzzaman & Sun, 2016; Liu, Sun, & Zeng, 2014). Regression models with selected wavelengths were used for building the adulteration map of samples.

2.5.2. *Adulteration map*

NIR-HSI has the advantage of visualising the distribution of the prediction model values in the spatial domain (pixels) (Kamruzzaman et al., 2016). The PLSR model with the selected wavelengths was applied to predict the level of adulteration in each pixel of the chicken sample. The hyperspectral image at selected wavelengths was unfolded in a two-dimensional (2-D) matrix, so that each single-band image became a column vector. Each pixel in the image was multiplied by the regression coefficients obtained from the PLSR model. After multiplication, the resulting matrix was refolded to form a 2-D colour image with the same dimensions of the single band image. This process results in a prediction map that demonstrates the distribution of the adulteration in each pixel of the image. A linear colour scale was used to map the predicted

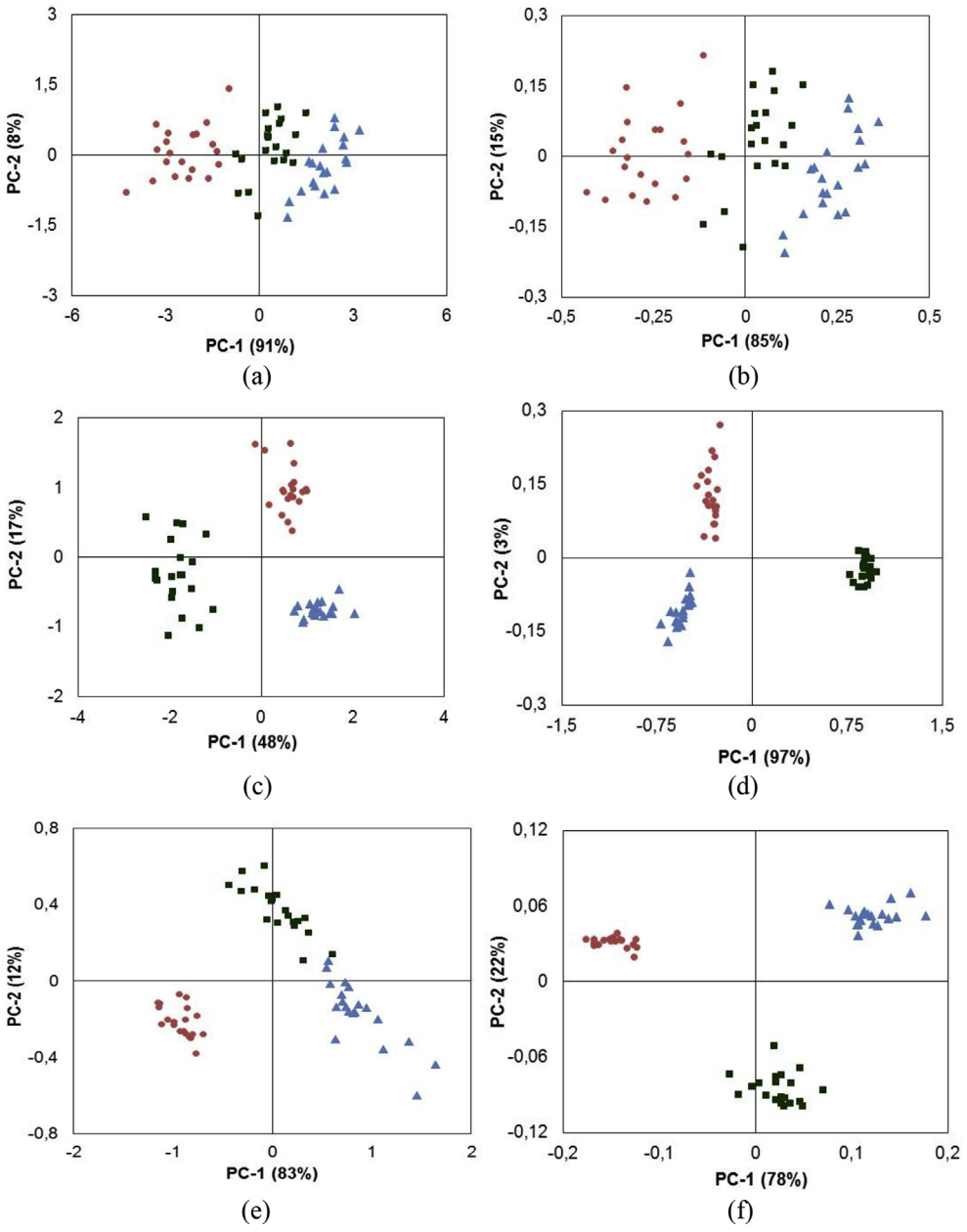

Fig. 2 – PCA scores for ground samples of different species: (■) beef, (•) pork and (▲) chicken. (a) PCA for full spectra acquired by portable NIR spectrometer; (b) PCA for three selected wavelengths from NIR spectrometer; (c) PCA for all features from RGB-I; (d) PCA for three selected features from RGB-I; (e) PCA for full spectra acquired by NIR-HSI; (f) PCA for three wavelengths selected from NIR-HSI.

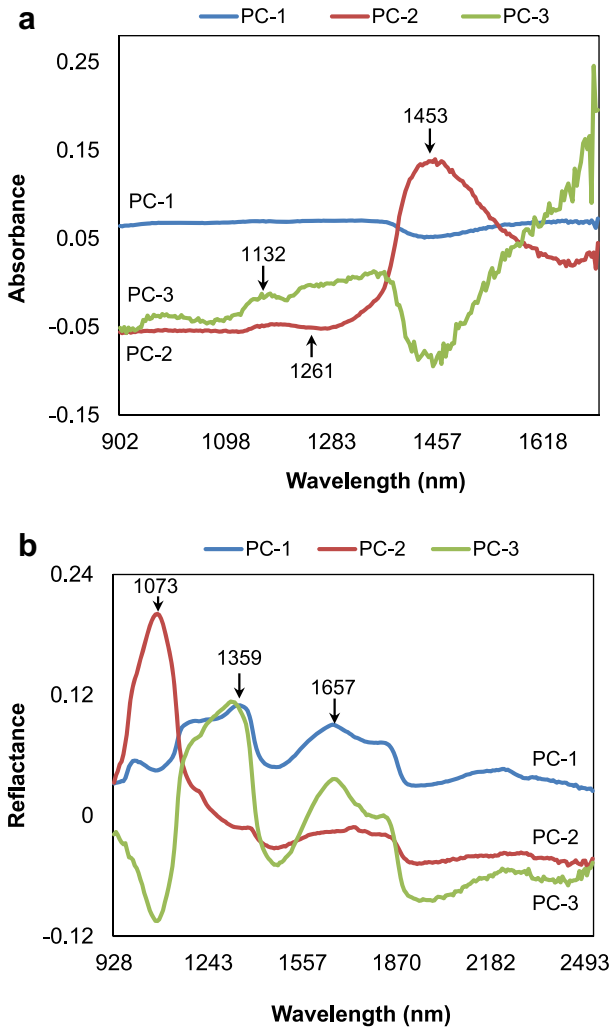

Fig. 3 – PCA loadings plot for ground samples of different species (a) spectra acquired by portable NIR spectrometer; (b) spectra acquired by NIR-HSI.

values of each pixel in different colours, where the colours represent different concentrations of the expected adulteration (Barbin, ElMasry, Sun, Allen, & Morsy, 2013; Kamruzzaman et al., 2016).

3. Results and discussion

3.1. *Spectral analyses*

The average NIRS spectra (900–1700 nm) in absorbance mode and NIR-HSI (900–2500 nm) in absorbance mode from chicken, beef and pork present similar trends across the NIR range 900–1700 nm (Fig. 1a and b). The characteristic bands of 970 nm and 1450 nm are related to 2nd and 1st overtone O–H stretching of water (Nolasco Perez et al., 2018; Xiong et al., 2015) and 1195 nm is related to the second overtone of CH_3 stretching (De Marchi, Riovanto, Penasa, & Cassandro, 2012). Specifically on the NIR-HSI spectra, the wavelength 1670 nm is related to the first overtone of the C–H stretching (Budić- Leto et al., 2011).

3.2. *Classification of ground meat*

PCA scores were used to visualise samples with similar spectral signatures (Fig. 2a–c). The first three principal components were responsible for 99.1% (portable NIR spectrometer), 74.0% (RGB-I), and 99.4% (NIR-HSI) of the total variance among the samples examined. Also, it is possible to observe that the samples did not overlap, showing a clear separation of the three species of ground meat. In addition, the loadings of the NIR data (Fig. 3a, b) were used to select important wavelengths. Regarding RGB-I, the variables were selected from the regression coefficients of PLSR models with highest modulus.

Figure 2d–f show PCA scores using, respectively, selected wavelengths 1132 nm, 1261 nm, 1453 nm for NIR spectrometer; 1073 nm, 1359 nm and 1657 nm for NIR-HSI; arithmetic mean of H, V and L* selected from RGB-I. It is possible to observe that the three classes are separate, with the first three main components responsible for 100% of the total variance among the samples examined for the three techniques, increasing its representativeness with respect to the PCA performed using all variables. Next, we performed the classification model based on the LDA algorithm using the data set of the ground meat samples.

Results for LDA of the three classes (chicken, beef, pork) reached an overall accuracy of 100%, with sensitivity and specificity of 1.00 for the ground meat data set of the three

Table 1 – Results for PLSR models for chicken samples adulterated with pork.

Technology	Pre-treatment	LV	Calibration				Validation			
			R_c^2	R_{cv}^2	RMSEC	RMSECV	R_p^2	RMSEP	RPD	RER
Portable NIR spectrometer	None	5	0.56	0.38	13.58	16.20	0.28	20.32	0.96	4.92
	SNV	5	0.48	0.24	14.66	17.91	0.02	23.79	0.82	4.20
	MSC	5	0.48	0.24	14.71	17.95	0.01	23.90	0.82	4.18
	1st der.	7	0.69	0.42	11.40	15.68	0.18	21.77	0.90	4.59
	2nd der.	1	0.16	0.10	18.76	19.59	0.13	22.38	0.88	4.47
NIR-HSI	None	8	0.94	0.83	5.18	8.61	0.83	10.00	1.96	10.00
	SNV	7	0.94	0.81	5.00	8.87	0.77	11.58	1.69	8.64
	MSC	7	0.94	0.82	4.90	8.40	0.77	11.58	1.69	8.64
	1st der.	6	0.91	0.87	6.16	7.44	0.80	10.65	1.84	9.39
	2nd der.	6	0.90	0.80	6.32	9.17	0.84	9.51	2.66	10.52
RGB-I	None	59	0.90	0.86	6.31	7.57	0.60	15.67	1.25	6.38

Table 2 – Results for PLSR models for chicken samples adulterated with beef.

Technique	Pre-treatment	LV	Calibration				Validation			
			R_c^2	R_{cv}^2	RMSEC	RMSECV	R_p^2	RMSEP	RPD	RER
Portable NIR spectrometer	–	12	0.93	0.82	5.48	8.08	0.67	13.81	1.42	7.24
	SNV	11	0.92	0.71	5.92	11.12	0.59	15.29	1.28	6.54
	MSC	11	0.91	0.67	6.05	11.89	0.59	15.28	1.28	6.54
	First derivate	9	0.92	0.82	5.87	8.74	0.70	13.07	1.50	7.65
	Second derivate	13	0.92	0.46	5.68	15.15	0.33	19.72	0.99	5.07
NIR–HSI	–	6	0.98	0.97	2.82	3.47	0.94	5.51	3.56	18.15
	SNV	5	0.97	0.96	3.18	3.73	0.93	6.50	3.01	15.38
	MSC	5	0.97	0.96	3.18	3.76	0.93	6.50	3.01	15.38
	First derivate	5	0.96	0.95	2.81	3.09	0.87	8.27	2.37	12.09
	Second derivate	5	0.97	0.95	2.65	3.7	0.78	10.71	1.83	9.34
RGB-I	–	59	0.96	0.94	4.11	4.86	0.90	7.67	2.56	13.04

types of species (chicken, beef and pork), for the three techniques used. The results of LDA confirmed the good performance of the classification of ground meats for different species, which is consistent with previous studies carried out by Rady and Adedeji (2018), using Vis/NIR and NIR spectroscopy.

3.3. *Prediction of adulteration in ground chicken samples*

In this section, the techniques were investigated to predict the concentration of pork or beef in ground chicken meat. Thus, NIR spectroscopy, NIR-HSI and RGB-I information were used as predictors for PLSR models. For NIR and NIR-HSI data, the calibration models were developed using raw and pre-processed spectra, separately (MSC, SNV, 1st derivative, 2nd derivative). Regression models using raw data provided good results to quantify beef in chicken meat using portable NIR spectrometer. However, the results with this spectrometer for prediction of pork adulteration in chicken samples were less accurate, maybe due to the small size of the sample area analysed in comparison to the imaging techniques (NIR-HSI or RGB-I) where the total area of the sample is assessed (Pasquini, 2018).

The results are presented for calibration and validation models (Tables 1 and 2). According to De Girolamo, Lippolis, Nordkvist, and Visconti (2009), R^2 values from 0.66 to 0.81

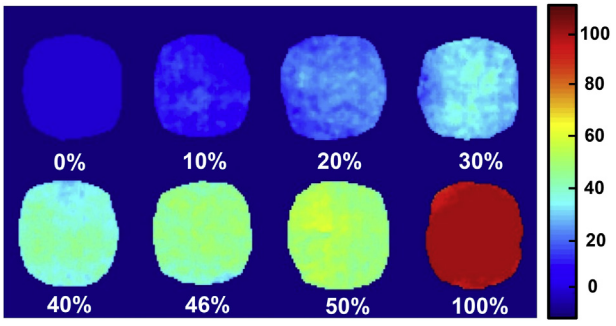

Fig. 4 – Prediction map for ground chicken samples adulterated with different percentages of beef.

Table 3 – Results for PLSR models with selected features for chicken samples adulterated with beef and pork.

Samples		LV	Wavelengths	Calibration				Prediction			
				R_c^2	R_{cv}^2	RMSEC	RMSECV	R_p^2	RMSEP	RPD	RER
Hyperspectral imaging											
Chicken and pork	PLSR	4	960, 1054, 1218, 1268, 1356	0.87	0.87	7.20	7.45	0.84	9.53	2.54	10.49
	Stepwise	5	979, 1048, 1218, 1262, 1306	0.86	0.85	7.49	7.88	0.83	9.98	2.43	10.17
Chicken and beef	PLSR	3	1067, 1187, 1444	0.95	0.95	4.05	4.20	0.92	6.34	3.82	15.77
	Stepwise	3	1073, 1105, 1300	0.96	0.96	3.61	3.76	0.91	6.89	3.51	14.51
Portable NIR spectrometer											
Chicken and pork	PLSR	4	977, 1013, 1195, 1280, 1476	0.45	0.41	15.21	15.93	0.39	18.68	1.3	5.35
	Stepwise	3	977, 1055, 1496, 1640, 1682	0.32	0.27	17.04	17.55	0.35	19.42	1.25	5.15
Chicken and beef	PLSR	4	1086, 1195, 1290, 1368, 1470	0.75	0.74	10.22	10.79	0.64	14.37	1.68	6.96
	Stepwise	5	977, 1079, 1269, 1382, 1406	0.79	0.78	9.35	9.80	0.66	13.99	1.73	7.15
RGB imaging											
Chicken and pork	PLSR	2	GLCM G Energy Mean a*, Mean b*	0.84	0.83	8.07	8.39	0.82	10.16	2.38	9.84
Chicken and beef	PLSR	2	Mean G, Mean BW Mean L*	0.96	0.96	3.90	4.04	0.86	9.10	2.66	10.99

LV – latent variable; GLCM G energy – gray level co-occurrence matrix G energy; mean a*– arithmetic mean of colour channel a*; mean b* – arithmetic mean of colour channel b*; mean G – arithmetic mean of colour channel G; mean BW – arithmetic mean of the binary image intensity; mean L* – arithmetic mean of colour channel L*

would allow the approximate quantitative prediction, while R^2 between 0.82 and 0.90 would allow a good prediction and R^2 higher than 0.91 would provide an excellent model.

In addition, the models were evaluated based on RPD and RER in order to verify the capacity and ability of the models. RPD values in the range 1.8–2.0 indicate that the model is good, and quantitative predictions are possible; 2.0–2.5 indicate that the model is very good and larger than 2.5 indicates that model is excellent (Kamruzzaman et al., 2016). RER values of less than 3 indicate little practical utility, RER between 3 and 10 indicate that the models are limited to good practical utility and RER greater than 10 indicate high accuracy (De Marchi et al., 2011; Jiang, Yoon, Zhuang, & Wang, 2017).

Therefore, the best results were obtained for NIR–HSI-based models to quantify pork or beef in chicken meat ($R_p^2 = 0.83$ and $R_p^2 = 0.94$, respectively), compared to RGB-I and NIR spectroscopy. For RGB-I technique ($R_p^2 = 0.90$) the model was good for quantification of beef in chicken meat. The results for portable NIR spectrometer ($R_p^2 = 0.67$) for quantification of beef or pork in chicken meat presented high values of RMSEP and RPD lower than 2.5, indicating they were not adequate for prediction.

The results of RPD and RER for NIR-HSI were 3.56 and 18.15 and for RGB-I were 2.56 and 13.04, respectively, indicating the models were excellent for predicting the level of beef in chicken samples. Overall, best results were obtained for identification of the presence of beef, than pork. Regarding the techniques, NIR-HSI was more accurate than NIR spectroscopy, probably due to the small region of measurement for the spectrometer. The limited sampling area of NIR spectroscopy instruments may represent a disadvantage that NIR-HSI is able to solve, since the region of interest for this application usually includes the entire sample.

3.4. *Prediction of adulteration in chicken samples using selected wavelengths*

In order to improve, optimise and reduce the size and time of data processing, a few selected wavelengths and/or image features were used to develop optimised PLSR models (Table 3). The validation model with the selected wavelengths was more accurate and robust than the models on full wavelengths due to the elimination of noise and variables with redundant information. The values of the quadratic calibration and cross-calibration errors showed little difference between them, which is indicative of good performance of the models. The coefficient of prediction (R_p^2) was 0.66 using the portable NIR spectrometer for chicken samples adulterated with beef, which indicates the possibility of using this instrument in the detection of adulterated chicken samples.

Values for RMSEC, RMSECV and RMSEP were high, but similar to previous studies. Zheng et al. (2019) obtained similar values for RMSEP, using NIR-HSI for prediction of adulteration of duck meat in minced lamb. López-Maestresalas et al. (2019) obtained better results for identification of chicken meat mixed with beef, than pork mixed with beef, using NIR spectroscopy, depending on the spectral pre-processing technique used. Kamruzzaman et al. (2016) found RPD values similar to the current study, for prediction of chicken adulteration in beef using NIR-HSI. In general, NIR-HSI provided better results for identification of meat adulteration, compared to NIR spectroscopy. This was also observed in the current work. The limited sampling area of NIR spectroscopy instruments may represent a disadvantage that NIR-HSI is able to solve, since the region of interest for this application usually includes the entire sample.

On the other hand, for NIR-HSI and RGB-I, the values in the coefficient of prediction were $R_p^2 = 0.84$ and $R_p^2 = 0.82$ respectively, with RPD and RER values of 2.54 and 10.49, respectively, for NIR-HSI, and 2.38 and 9.84, respectively, for RGB-I. This indicates that the models were good in predicting the levels of the admixtures of pork in chicken samples. For chicken meat samples adulterated with beef, RPD and RER values were 3.82 and 15.77 for NIR-HSI, respectively, and for RGB-I the RPD and RER values were 2.66 and 10.99 respectively. According to Wold, Jakobsen, and Krane (1996), in some cases the multivariate prediction model may improve with the selection of important variables, similar to reported in this research for NIR-HSI.

3.5. *Prediction map*

The optimised model with selected wavelengths was transferred to each pixel of the image, where the different adulteration levels from lowest to highest percentage were presented in different colours (Fig. 4). As can be observed, hyperspectral imaging has the advantage of allowing the visualisation of the concentration of adulteration when compared to the portable NIR technique, thus providing information about the homogeneity of the mixtures. However, the RGB-I has also provided considerable results that can be used in the meat processing industry.

4. Conclusion

This research compared the results of three different approaches for classification of ground meat from different species and quantification of adulteration by pork and beef in ground chicken meat. Portable NIR spectrometer, NIR-HSI and RGB-I system were able to classify the ground meats with different levels of accuracy. Further, data processing was optimised with the reduction of variables, obtaining 100% classification of chicken, pork and beef samples using Linear Discriminant Analysis. PLSR models confirmed that NIR-HSI provided the best results among these techniques for quantification of beef and pork added to chicken meat, and could be a fast and non-invasive tool for meat inspection. These techniques could provide alternatives to the meat processing industry, according to the cost of equipment and objective of the analysis to be performed.

Acknowledgement

This study was financed in part by the Coordenação de Aperfeiçoamento de Pessoal de Nível Superior – Brasil (CAPES) – Finance Code 001. Irene Marivel Nolasco Pérez acknowledges Coordination for the Improvement of Higher Education

Personnel (CAPES) for the scholarship. The authors acknowledge the Brazilian National Council for Scientific and Technological Development (CNPq) (Grant no. 404852/2016-5), São Paulo Research Foundation (FAPESP), Young Researchers Award (Grant no. 2015/24351-2); FAPESP Grant no. 2008/57808-1 and 2014/50951-4; CNPq Grant no. 465768/2014-8. The authors kindly acknowledge the support provided by Mrs. Cristiane Vidal during NIR-HSI system operation and data processing.

REFERENCES

Alamprese, C., Amigo, J. M., Casiraghi, E., & Engelsen, S. B. (2016). Identification and quantification of Turkey meat adulteration in fresh, frozen-thawed and cooked minced beef by FT-NIR spectroscopy and chemometrics. *Meat Science, 121*, 175–181. https://doi.org/10.1016/J.MEATSCI.2016.06.018.

Arsalane, A., El Barbri, N., Rhofir, K., Tabyaoui, A., & Klilou, A. (2017). Beef and horse meat discrimination and storage time classification using a portable device based on DSP and PCA method. *International Journal of Intelligent Enterprise, 4*(1–2), 58–75. https://doi.org/10.1504/IJIE.2017.087005.

Arsalane, A., El Barbri, N., Tabyaoui, A., Klilou, A., Rhofir, K., & Halimi, A. (2018). An embedded system based on DSP platform and PCA-SVM algorithms for rapid beef meat freshness prediction and identification. *Computers and Electronics in Agriculture, 152*(July), 385–392. https://doi.org/10.1016/j.compag.2018.07.031.

Ballin, N. Z. (2010). Authentication of meat and meat products. *Meat Science, 86*(3), 577–587. https://doi.org/10.1016/J.MEATSCI.2010.06.001.

Ballin, N. Z., Vogensen, F. K., & Karlsson, A. H. (2009). Species determination – can we detect and quantify meat adulteration? *Meat Science, 83*(2), 165–174. https://doi.org/10.1016/J.MEATSCI.2009.06.003.

Barbin, D. F., ElMasry, G., Sun, D.-W., Allen, P., & Morsy, N. (2013). Non-destructive assessment of microbial contamination in porcine meat using NIR hyperspectral imaging. *Innovative Food Science & Emerging Technologies, 17*, 180–191. https://doi.org/10.1016/j.ifset.2012.11.001.

Barbin, D. F., Kaminishikawahara, C. M., Soares, A. L., Mizubuti, I. Y., Grespan, M., Shimokomaki, M., et al. (2015). Prediction of chicken quality attributes by near infrared spectroscopy. *Food Chemistry, 168*, 554–560. https://doi.org/10.1016/J.FOODCHEM.2014.07.101.

Barbin, D. F., Mastelini, S. M., Barbon, S., Campos, G. F. C., Barbon, A. P. A. C., & Shimokomaki, M. (2016). Digital image analyses as an alternative tool for chicken quality assessment. *Biosystems Engineering, 144*, 85–93. https://doi.org/10.1016/j.biosystemseng.2016.01.015.

Barreto, A., Cruz-Tirado, J. P., Siche, R., & Quevedo, R. (2018). Determination of starch content in adulterated fresh cheese using hyperspectral imaging. *Food Bioscience, 21*, 14–19. https://doi.org/10.1016/J.FBIO.2017.10.009.

Budić- Leto, I., Gajdoš, J., Zduni, G., Tomi, I., Banovi, M., Kurtanjek, Ž., et al. (2011). Usefulness of near infrared spectroscopy and chemometrics in screening of the quality of dessert wine Prošek. *Croatian Journal of Food Science and Technology, 3*(2), 9–15.

Campos, M. I., Mussons, M. L., Antolin, G., Debán, L., & Pardo, R. (2017). On-line prediction of sodium content in vacuum packed dry-cured ham slices by non-invasive near infrared spectroscopy. *Meat Science, 126*, 29–35. https://doi.org/10.1016/J.MEATSCI.2016.12.005.

Cluff, K., Naganathan, G. K., Subbiah, J., Lu, R., Calkins, C. R., & Samal, A. (2008). Optical scattering in beef steak to predict tenderness using hyperspectral imaging in the VIS-NIR region. *Sensing and Instrumentation for Food Quality and Safety, 2*(3), 189–196. https://doi.org/10.1007/s11694-008-9052-2.

De Girolamo, A., Lippolis, V., Nordkvist, E., & Visconti, A. (2009). Rapid and non-invasive analysis of deoxynivalenol in durum and common wheat by Fourier-Transform Near Infrared (FT-NIR) spectroscopy. *Food Additives & Contaminants Part A Chemistry, Analysis, Control, Exposure and Risk Assessment, 26*(6), 907–917. https://doi.org/10.1080/02652030902788946.

De Marchi, M., Penasa, M., Battagin, M., Zanetti, E., Pulici, C., & Cassandro, M. (2011). Feasibility of the direct application of near-infrared reflectance spectroscopy on intact chicken breasts to predict meat color and physical traits. *Poultry Science, 90*(7). https://doi.org/10.3382/ps.2010-01239.

De Marchi, M., Riovanto, R., Penasa, M., & Cassandro, M. (2012). At-line prediction of fatty acid profile in chicken breast using near infrared reflectance spectroscopy. *Meat Science, 90*(3), 653–657. https://doi.org/10.1016/J.MEATSCI.2011.10.009.

Feng, C.-H., Makino, Y., Oshita, S., & Garcia-Martin, J. F. (2018). Hyperspectral imaging and multispectral imaging as the novel techniques for detecting defects in raw and processed meat products: Current state-of-the-art research advances. *Food Control, 84*, 165–176.

Feng, C.-H., Makino, Y., Yoshimura, M., Thuyet, D. Q., Oshita, S., & Garcia-Martin, J. F. (2018). Hyperspectral imaging in tandem with R statistics and image processing for detection and visualization of pH in Japanese big sausages under different storage conditions. *Journal of Food Science, 83*(2), 358–366.

Fernandes, D. D. de S., Romeo, F., Krepper, G., Di Nezio, M. S., Pistonesi, M. F., Centurión, M. E., et al. (2019). Quantification and identification of adulteration in the fat content of chicken hamburgers using digital images and chemometric tools. *LWT, 100*, 20–27. https://doi.org/10.1016/J.LWT.2018.10.034.

Garcia-Martin, J. F. (2015). Optical path length and wavelength selection using Vis/NIR spectroscopy for olive oil's free acidity determination. *International Journal of Food Science and Technology, 50*, 1461–1467.

Grunert, T., Stephan, R., Ehling-Schulz, M., & Johler, S. (2016). Fourier Transform Infrared Spectroscopy enables rapid differentiation of fresh and frozen/thawed chicken. *Food Control, 60*, 361–364. https://doi.org/10.1016/j.foodcont.2015.08.016.

Jiang, H., Yoon, S.-C., Zhuang, H., & Wang, W. (2017). Predicting color traits of intact broiler breast fillets using visible and near-infrared spectroscopy. *Food Analytical Methods, 10*(10), 3443–3451. https://doi.org/10.1007/s12161-017-0907-1.

Kamruzzaman, M., ElMasry, G., Sun, D.-W., & Allen, P. (2012). Prediction of some quality attributes of lamb meat using near-infrared hyperspectral imaging and multivariate analysis. *Analytica Chimica Acta, 714*, 57–67. https://doi.org/10.1016/J.ACA.2011.11.037.

Kamruzzaman, M., Makino, Y., & Oshita, S. (2016). Rapid and non-destructive detection of chicken adulteration in minced beef using visible near-infrared hyperspectral imaging and machine learning. *Journal of Food Engineering, 170*, 8–15. https://doi.org/10.1016/J.JFOODENG.2015.08.023.

Kamruzzaman, M., & Sun, D.-W. (2016). Introduction to hyperspectral imaging technology. In *Computer vision technology for food quality evaluation* (pp. 111–139). Elsevier. https://doi.org/10.1016/B978-0-12-802232-0.00005-0.

Li, X., Feng, F., Gao, R., Wang, L., Qian, Y., Li, C., et al. (2016). Application of near infrared reflectance (NIR) spectroscopy to identify potential PSE meat. *Journal of the Science of Food and Agriculture, 96*(9). https://doi.org/10.1002/jsfa.7493.

Liu, J.-H., Sun, X., Young, J. M., Bachmeier, L. A., & Newman, D. J. (2018). Predicting pork loin intramuscular fat using computer vision system. *Meat Science, 143*, 18–23. https://doi.org/10.1016/J.MEATSCI.2018.03.020.

Liu, D., Sun, D.-W., & Zeng, X.-A. (2014). Recent advances in wavelength selection techniques for hyperspectral image processing in the food industry. *Food and Bioprocess Technology, 7*(2), 307–323. https://doi.org/10.1007/s11947-013-1193-6.

López-Maestresalas, A., Insausti, K., Jarén, C., Pérez Roncal, C., Urrutia, O., Beriain, M. J., et al. (2019). Detection of minced lamb and beef fraud using NIR spectroscopy. *Food Control, 98*, 465–473.

Martínez Gila, D. M., Cano Marchal, P., Gámez García, J., & Gómez Ortega, J. (2015). On-line system based on hyperspectral information to estimate acidity, moisture and peroxides in olive oil samples. *Computers and Electronics in Agriculture, 116*, 1–7. https://doi.org/10.1016/J.COMPAG.2015.06.002.

Massantini, R., Raponi, F., Monarca, D., Ferri, S., Moscetti, R., Liang, P., et al. (2017). Real-time monitoring of organic carrot (var. Romance) during hot-air drying using near-infrared spectroscopy. *Food and Bioprocess Technology, 10*(11), 2046–2059. https://doi.org/10.1007/s11947-017-1975-3.

Mora, A. D., & Fonseca, J. M. (2014). Metodologia para a deteção de artefactos luminosos em imagens de retinografia com aplicação em rastreio oftalmológico. *RISTI: Revista Ibérica de Sistemas e Tecnologias de Informação*, (13), 51–63. https://doi.org/10.4304/risti.13.51-63.

Munir, M. T., Wilson, D. I., Depree, N., Boiarkina, I., Prince-Pike, A., & Young, B. R. (2017). Real-time product release and process control challenges in the dairy milk powder industry. *Current Opinion in Food Science, 17*, 25–29. https://doi.org/10.1016/J.COFS.2017.08.005.

Nolasco Perez, I. M., Badaró, A. T., Barbon, S., Barbon, A. P. A., Pollonio, M. A. R., & Barbin, D. F. (2018). Classification of chicken parts using a portable near-infrared (NIR) spectrophotometer and machine learning. *Applied Spectroscopy, 0*(0). https://doi.org/10.1177/0003702818788878, 370281878887.

Otsu, N. (1979). A tlreshold selection method from gray-level histograms. *IEEE Transactions on Systems, Man, and Cybernetics, 9*(1), 62–66. https://doi.org/10.1109/TSMC.1979.4310076.

Pasquini, C. (2018). Near infrared spectroscopy: A mature analytical technique with new perspectives – A review. *Analytica Chimica Acta, 1026*, 8–36. https://doi.org/10.1016/J.ACA.2018.04.004.

Pizarro, C., Rodríguez-Tecedor, S., Pérez-del-Notario, N., Esteban-Díez, I., & González-Sáiz, J. M. (2013). Classification of Spanish extra virgin olive oils by data fusion of visible spectroscopic fingerprints and chemical descriptors. *Food Chemistry, 138*(2–3), 915–922. https://doi.org/10.1016/J.FOODCHEM.2012.11.087.

Prieto, N., Juárez, M., Larsen, I. L., López-Campos, Ó., Zijlstra, R. T., & Aalhus, J. L. (2015). Rapid discrimination of enhanced quality pork by visible and near infrared spectroscopy. *Meat Science, 110*. https://doi.org/10.1016/j.meatsci.2015.07.006.

Rady, A., & Adedeji, A. (2018). Assessing different processed meats for adulterants using visible-near-infrared spectroscopy. *Meat Science, 136*, 59–67. https://doi.org/10.1016/J.MEATSCI.2017.10.014.

Riccioli, C., Pérez-Marín, D., & Garrido-Varo, A. (2018). Identifying animal species in NIR hyperspectral images of processed animal proteins (PAPs): Comparison of multivariate techniques. *Chemometrics and Intelligent Laboratory Systems, 172*, 139–149. https://doi.org/10.1016/J.CHEMOLAB.2017.12.003.

Santos Pereira, L. F., Barbon, S., Valous, N. A., & Barbin, D. F. (2018). Predicting the ripening of papaya fruit with digital imaging and random forests. *Computers and Electronics in Agriculture, 145*, 76–82. https://doi.org/10.1016/J.COMPAG.2017.12.029.

Santos, João Rodrigo, Viegas, Olga, Páscoa, Ricardo N. M. J., Ferreira, Isabel M. P. L. V. O., Rangel, António O. S. S., & Lopes, João Almeida (2016). In-line monitoring of the coffee roasting process with near infrared spectroscopy: Measurement of sucrose and colour. *Food Chemistry, 208*, 103–110. https://doi.org/10.1016/J.FOODCHEM.2016.03.114.

Sun, X., Young, J., Liu, J.-H., & Newman, D. (2018). Prediction of pork loin quality using online computer vision system and artificial intelligence model. *Meat Science, 140*, 72–77. https://doi.org/10.1016/J.MEATSCI.2018.03.005.

Wang, W., Peng, Y., Sun, H., Zheng, X., & Wei, W. (2018). Real-time inspection of pork quality attributes using dual-band spectroscopy. *Journal of Food Engineering, 237*, 103–109. https://doi.org/10.1016/J.JFOODENG.2018.05.022.

Wold, J. P., Jakobsen, T., & Krane, L. (1996). Atlantic salmon average fat content estimated by near-infrared transmittance spectroscopy. *Journal of Food Sciencie, 61*(1), 74–77.

Woolfe, M., & Primrose, S. (2004). Food forensics: Using DNA technology to combat misdescription and fraud. *Trends in Biotechnology, 22*(5), 222–226. https://doi.org/10.1016/J.TIBTECH.2004.03.010.

Xiong, Z., Sun, D.-W., Xie, A., Pu, H., Han, Z., & Luo, M. (2015). Quantitative determination of total pigments in red meats using hyperspectral imaging and multivariate analysis. *Food Chemistry, 178*, 339–345. https://doi.org/10.1016/j.foodchem.2015.01.071.

Yang, Y., Zhuang, H., Yoon, S.-C., Wang, W., Jiang, H., & Jia, B. (2018). Rapid classification of intact chicken breast fillets by predicting principal component score of quality traits with visible/near-infrared spectroscopy. *Food Chemistry, 244*, 184–189. https://doi.org/10.1016/J.FOODCHEM.2017.09.148.

Zheng, X., Li, Y., Wei, W., & Peng, Y. (2019). Detection of adulteration with duck meat in minced lamb meat by using visible near-infrared hyperspectral imaging. *Meat Science, 149*, 55–62. https://doi.org/10.1016/J.MEATSCI.2018.11.005.